processes

MDPI

Article

Numerical Investigation on Coal Combustion in Ultralow CO_2 Blast Furnace: Effect of Oxygen Temperature

Zhenfeng Zhou [1,*], Qiujie Yi [1], Ruihao Wang [1], Guang Wang [2] and Chunyuan Ma [3]

[1] College of Mechanical and Electronic Engineering, Shandong University of Science and Technology, Qingdao 266590, China; yiqiujie@163.com (Q.Y.); w1320787264@163.com (R.W.)
[2] State Key Laboratory of Advanced Metallurgy, University of Science and Technology Beijing, Beijing 100083, China; wangguang@ustb.edu.cn
[3] National Engineering Laboratory of Coal-Fired Pollution Reduction, Shandong University, Jinan 250061, China; sdetechym@163.com
* Correspondence: zhouzhenfeng@sdust.edu.cn; Tel.: +86-0532-86057685

Received: 28 June 2020; Accepted: 17 July 2020; Published: 20 July 2020

Abstract: The cooling effect of room-temperature oxygen in oxygen blast furnaces with top gas recycling (TGR-OBF) delays the coal combustion process. To further explore the oxygen–coal combustion mechanism and intensify coal combustion in TGR-OBF, the effect of oxygen temperature on coal combustion was investigated using computational fluid dynamics (CFD). A three-dimensional model was developed to simulate the lance–blowpipe–tuyere–raceway of TGR-OBF. The effect of oxygen temperature at the same oxygen velocity and mass flow on coal combustion was investigated. Results showed the cooling effect of room-temperature oxygen was weakened, and the coal burnout was greatly increased with the increase in oxygen temperature. In particular, the coal burnout increased from 21.64% to 81.98% at the same oxygen velocity when the oxygen temperature increased from 300 to 500 K. The results provide useful reference for the development of TGR-OBF and coal combustion technology.

Keywords: TGR-OBF; raceway; oxygen temperature; coal; burnout

1. Introduction

Blast furnaces are the main facilities to produce hot metal because of their high productivity and competitive cost compared to other ironmaking technologies [1–4]. However, the production process of hot metal consumes a lot of fossil fuel and produces significant amounts of CO_2. Therefore, there is great environmental concern about blast furnaces, and it is necessary to further conserve energy and reduce CO_2 emissions. It is hard to significantly change carbon consumption and CO_2 emissions under the present conditions. Consequently, there is a need to develop a new process of blast furnace, and this is also key to maintaining the use of blast furnaces.

Oxygen blast furnace with top gas recycling (TGR-OBF) is a new blast furnace process, representing the development direction of blast furnaces [5–8]. A schematic diagram of the TGR-OBF process is shown in Figure 1a. Compared to the traditional blast furnace (TBF) (shown in Figure 1b), room-temperature oxygen is injected in TGR-OBF instead of hot air. Furthermore, the CO_2-stripped top gas is heated and recycled into the blast furnace. In theory, the CO_2 emission and carbon consumption of TGR-OBF can be reduced by 76% and 24%, respectively, compared to TBF [9]. The CO_2 concentration in the top gas of TGR-OBF also increases significantly, which is very beneficial for the removal of CO_2 in top gas. Furthermore, the main component of top gas is CO and CO_2, and it can be used for the production of methanol [10–12]. Therefore, the additional value of top gas is enhanced.

The blast parameters of TGR-OBF change greatly compared to those of TBF, and the coal combustion characteristics will then also change significantly. Therefore, the crux of high pulverized coal rate (PCR) in TGR-OBF is to further reveal the coal combustion characteristics and then explore a proper solution to the problem.

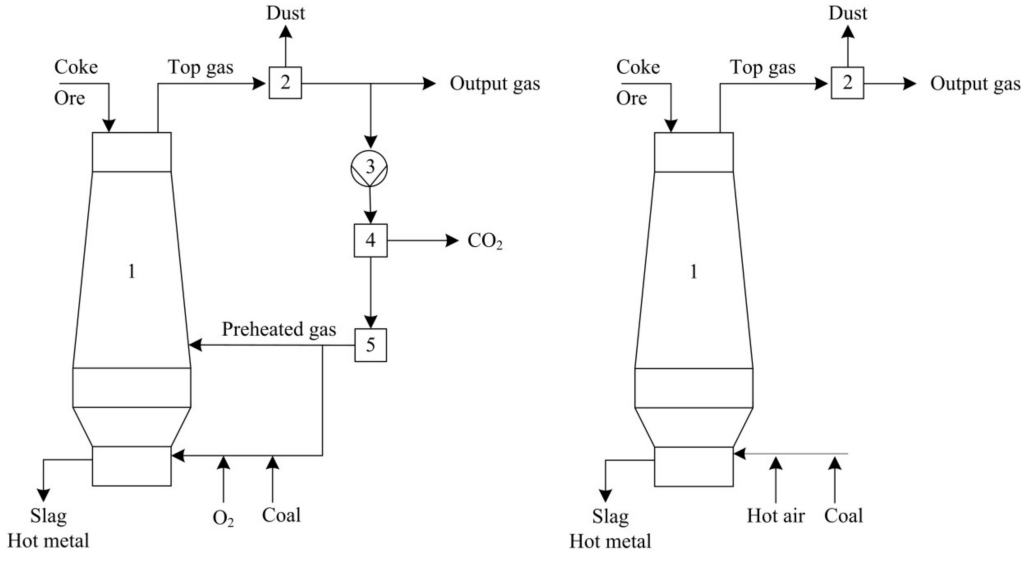

Figure 1. Schematic diagrams of (**a**) oxygen blast furnace with top gas recycling (TGR-OBF) and (**b**) traditional blast furnace (TBF).

In our previous work [13], the coal burnout at 70% O_2 was found to be only 21.64%. The coal burnout of TBF is 71.78%, meaning TGR-OBF does not have any advantage over TBF. Although the oxygen concentration in TGR-OBF increases significantly, the cooling effect of room-temperature oxygen has some adverse effect on coal combustion. The oxygen temperature may be the main reason causing this phenomena, so properly increasing it may be helpful for coal combustion.

Many investigations by other scholars have focused on the coal combustion of TBF. Shen et al. [14–16] investigated the effect of blast temperature and oxygen content on coal combustion in TBF. Chen et al. [17–19] investigated the effect of coal lance configurations on coal combustion in TBF. Sato et al. [6] discussed the next-generation ironmaking process based on TGR-OBF using a material and energy balance model. Sahu et al. [20,21] simulated the behavior of TGR-OBF under different operating conditions using a two-zone furnace model. However, investigations on coal combustion in TGR-OBF are lacking. Most of the current research remains in the theoretical stage, and there is still much deficiency in the understanding of TGR-OBF. Therefore, it is necessary to carry out further investigations on coal combustion in TGR-OBF. This will be beneficial for better understanding TGR-OBF. Furthermore, it will be helpful for the development of TGR-OBF.

It is very difficult to carry out a pulverized coal injection trial in a real or simulated blast furnace because of the hazardous environment and complex condition in the raceway region of the blast furnace. Fortunately, computational fluid dynamics (CFD) has become a powerful tool for the investigation of coal combustion in blast furnaces. Furthermore, the reliability and superiority of CFD have been fully proven by many scholars [15,17,22,23].

Considering the aforementioned reasons, in this study, a three-dimensional model was developed to simulate the lance–blowpipe–tuyere–raceway of a TGR-OBF. The effect of oxygen temperature at 70% O_2 on coal combustion was investigated. The effect of oxygen temperature at the same velocity and mass flow on coal combustion was also investigated. The results provide useful insight into the

development of the TGR-OBF process. Furthermore, it helps explore an effective way of intensifying coal combustion in TGR-OBF.

2. Mathematical Model

2.1. Basic Equations

The gas–particle flow and coal combustion in the tuyere and raceway regions were calculated based on the framework of software package ANSYS-FLUENT. The model formulations of the gas and particle phases have been described in our previous works in detail [24–26].

2.2. Combustion Process

Coal combustion is regarded as a multistage overlapping process consisting of (i) preheating, (ii) devolatilization of raw coal, (iii) combustion of volatiles, and (iv) oxidation/gasification of the residual char [27].

(1) Devolatilization of Coal

The devolatilization process releases volatiles ($C_\alpha H_\beta O_\gamma N_\delta$) and char ($C_{(s)}$). The coal devolatilization process is simulated using the so-called two competing reactions model. A pair of reactions with different rates (k_1, k_2) and volatile yields (α_1, α_2) compete to pyrolyze the raw coal.

$$\textit{Raw Coal} \begin{array}{l} k_1 \nearrow \alpha_1 VM_1 + (1-\alpha_1)C_1 \ (\textit{Low Temperature}) \\ k_2 \searrow \alpha_2 VM_2 + (1-\alpha_2)C_2 \ (\textit{High Temperature}) \end{array}$$

(2) Gas Combustion

The gas combustion reactions are as follows:

$$C_\alpha H_\beta O_\gamma N_\delta + aO_2 \rightarrow bCO + cH_2O + dN_2 \quad (1)$$

$$CO + 0.5O_2 \rightarrow CO_2 \quad (2)$$

$$C_\alpha H_\beta O_\gamma N_\delta + aO_2 \rightarrow bCO + cH_2O + dN_2 \quad (3)$$

In turbulent flow, the gas reaction mechanisms are represented by the finite rate/eddy dissipation model. The net reaction rate is determined by the chemistry rate and the mixing rate.

(3) Oxidation/Gasification of Residual Char

For the char reactions, the heterogeneous surface reaction model is used [28]. The following reactions are considered during the coal combustion process:

$$C(s) + 0.5O_2 \rightarrow CO \quad (4)$$

$$C(s) + CO_2 \rightarrow 2CO \quad (5)$$

$$C(s) + H_2O \rightarrow CO + H_2 \quad (6)$$

The reaction rate is expressed as follows:

$$R_{j,r} = A_p \eta_r Y_j P \frac{k_r D_{0,r}}{D_{0,r} + k_r}$$

where A_p and η_r indicate the particle surface area (m^2) and effectiveness factor, respectively; Y_j is the mass fraction of species j; and P represents the partial pressure (Pa).

3. Geometry and Operating Conditions

A test TGR-OBF of 120 m^3 was built based on a TBF of 120 m^3 at Laiwu Steel Company in Shandong Province, China. To further understand the operation of pulverized coal injection in TGR-OBF, the

coal combustion characteristics in TGR-OBF was investigated. The main operating parameters of the TGR-OBF and TBF are summarized in Tables 1 and 2. The properties of pulverized coal used in this model are shown in Table 3 [23].

Table 1. Main blast parameters of TBF.

Blast Volume (Nm^3/t)	Blast Temperature (K)	Volume (m^3)	Coal Ratio (kg/t)
1129	1473	120	150

Table 2. Main blast parameters of TGR-OBF.

Oxygen		Recycling Top Gas						
Volume Nm^3/t	Content %	Volume Nm^3/t	Temperature K	CO %	H_2 %	CO_2 %	N_2 %	H_2O %
366	70	280	1173	52.58	10.81	4.5	31.49	0.62

Table 3. Properties of coal [23].

Proximate Analysis (wt %)		Ultimate Analysis		Size Distribution
Moisture	1	C	88.78	90 μm: 5%
Volatiles	20.02	H	4.54	63 μm: 25%
Ash	8.32	O	4.68	45 μm: 55%
Fixed carbon	70.66	N	2	20 μm: 15%

The geometric details of the models are shown in Figure 2. The models simulated the lance–blowpipe–tuyere–raceway of blast furnaces. The coal particles mainly flowed along the horizontal direction in the raceway region. The coal burnout at the end of the raceway represented that of the entire raceway region. Therefore, the investigations were mainly focused on coal combustion along the horizontal direction. The 120 m^3 TBF was dissected in 2007. The dissection results showed the raceway depth to be about 700 mm. Therefore, the raceway was designed as a tube of 700 mm length with a divergence angle of 3° in accordance with others [27].

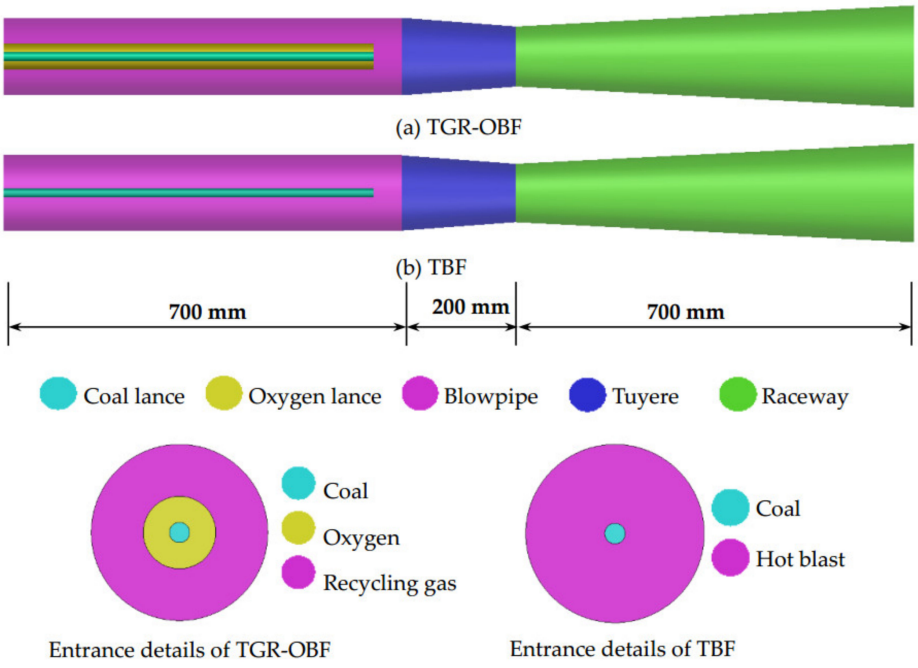

Figure 2. Geometric details of the models.

4. Results and Discussion

4.1. Model Validation

The coal combustion in blast furnaces or other facilities has been investigated by many scholars using CFD [17,28–32]. The reliability of CFD has been fully proven. Moreover, investigations on coal combustion in TBF has been carried out using CFD before investigating that in TGR-OBF [21–23]. The effect of the oxygen content in hot blast on coal combustion was investigated in our earlier work [24], and the results and phenomena were the same or similar to that of other scholars [27]. Furthermore, the cooling effect of room-temperature oxygen on coal combustion was illustrated in our earlier study [25], which was also in good agreement with the study by Chen [17]. These comparisons fully prove that the model is reliable. Therefore, it is completely acceptable to investigate coal combustion in TGR-OBF using this model.

4.2. Effect of Oxygen Temperature at the Same Velocity

First, the effect of oxygen temperature at the same velocity on coal combustion was investigated using the numerical model.

Figure 3a shows the effect of oxygen temperature on the final coal burnout at the raceway outlet. In general, the effect of oxygen temperature was very obvious. The coal burnout at 300 K was only 21.64%. When the oxygen temperature increased to 400 K, the coal burnout increased to 75.86%. The burnout at 500 K was 81.98%, which was the maximum. As oxygen temperature continued to increase, the coal burnout slightly decreased. The coal particles were in direct contact with the oxygen stream after leaving the coal lance. The cooling effect of room-temperature oxygen delayed the coal combustion process. The cold oxygen volume decreased with the increase in oxygen temperature. The adverse effect of cold oxygen was weakened, and the char had more time to react with oxygen. Figure 3b shows the changes in pure oxygen volume with oxygen temperature. The complete combustion of 150 kg/t·HM pulverized coal required 143.97 Nm^3 O_2. However, the pure oxygen volume at 300 K was 256.2 Nm^3/t·HM, which could fully meet coal combustion. The excess cold oxygen would be harmful for coal combustion. The pure oxygen volume at 400 and 600 K could both meet full combustion of 150 kg/t·HM pulverized coal. The pure oxygen volume at 600 K was 128.1 Nm^3/t·HM. This would not theoretically meet full combustion of 150 kg/t·HM pulverized coal. Furthermore, some oxygen would be used for recycling gas combustion. Therefore, the coal burnout slightly decreased. It can be concluded that properly decreasing the oxygen volume in direct contact with coal particles is very useful for coal combustion.

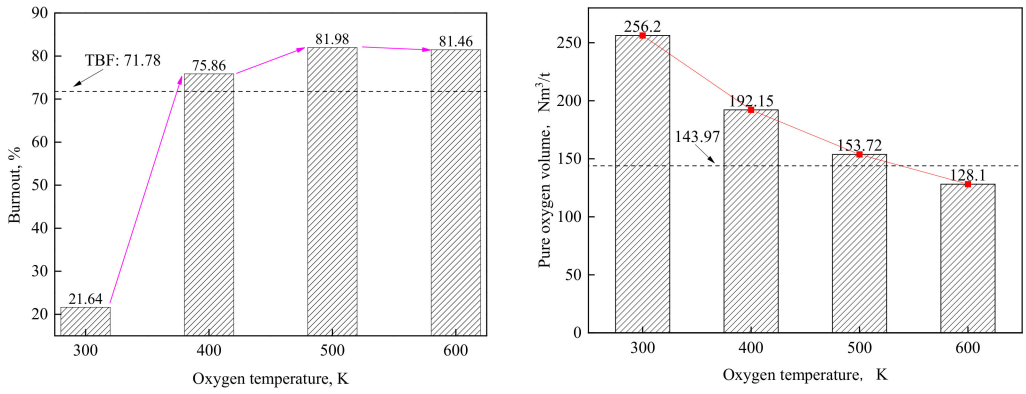

(a) (b)

Figure 3. Effect of oxygen temperature: (**a**) coal burnout; (**b**) pure oxygen amount, Nm^3/t·HM.

The coal burnout at different positions was investigated, as shown in Figure 4a. The coal combustion process was enhanced with increase in oxygen temperature. When the oxygen temperature

was 300 K, the coal particles only began to release volatiles at a distance of about 0.6 m. With the increase in oxygen temperature, the coal combustion process was enhanced. In particular, the coal particles already started to release volatiles at a distance of 0.4 m at 600 K oxygen temperature. If the devolatilization process was to be extended, the char combustion process would be shortened. Finally, the coal particles would leave the raceway region without full combustion. Significant devolatilization starts at about 600 K [28,33]. Figure 4b shows that the coal particles were rapidly heated with the increase in oxygen temperature. This was the main reason for the rapid combustion of coal particles with the increase in oxygen temperature. With the increase in oxygen temperature, the cold oxygen volume decreased, and the coal particles could get more heat. The heat was mainly from the recycling gas combustion in the initial combustion process, so the CO reaction rate of different oxygen temperatures was investigated, as shown in Figure 4c. With the increase in oxygen temperature, the CO reaction rate slightly increased before a distance of 0.4 m and rapidly increased after 0.4 m. In the raceway region, the mixing rate of oxygen and recycling gas was the limiting factor of CO reaction. The increase in temperature was useful for the mixing of oxygen and recycling gas.

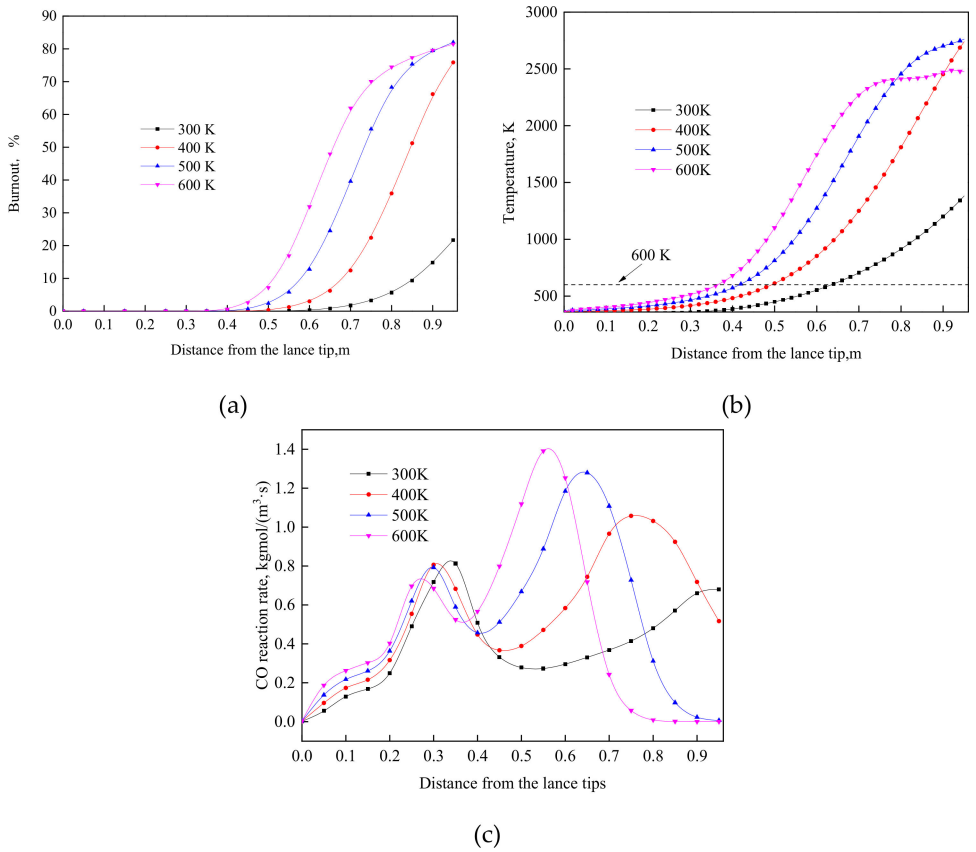

Figure 4. Effect of oxygen temperature: (**a**) coal burnout at different positions; (**b**) coal particle temperature at different positions; (**c**) CO reaction rate.

To better understand coal combustion characteristics under different oxygen temperatures, the mass ratio (m/m_0) of volatile matter was investigated, as shown in Figure 5. The mass ratio was defined as the ratio of char (or volatiles) mass in coal particles to that in raw coal particles. The devolatilization process was enhanced with the increase in oxygen temperature. This was in accordance with the change in coal particle temperature and burnout. Many of the coal particles still could not completely release volatiles at the raceway outlet when the oxygen temperature was 300 K. This was the main reason for a lower burnout under 300 K oxygen temperature. With the increase in oxygen temperature, more coal particles completely released volatiles. In particular, all the volatiles were released under 500 and 600 K oxygen temperature at the raceway outlet. Furthermore, the general devolatilization

rate increased with the increase in oxygen temperature. This was because the cold oxygen volume decreased, and the coal particles could obtain more heat. Furthermore, the recycling gas combustion reaction was intensified, and more heat was released. Promoting recycling gas combustion in the initial coal combustion stage is therefore key to increasing coal burnout.

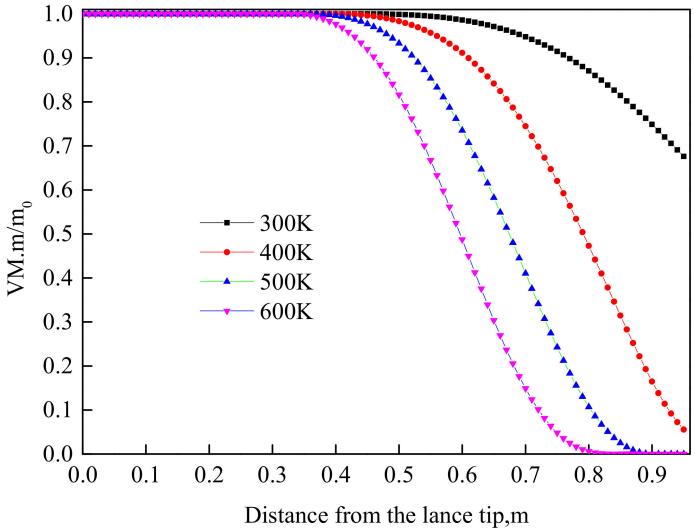

Figure 5. Effect of oxygen temperature on mass ratio (m/m_0) of volatile matter.

The volatile and char mass fraction were 22.08% and 77.92%, respectively, in combustibles. In other words, the volatiles only contributed a little and the char contributed a lot to the coal burnout. Therefore, to further reveal the effect of oxygen temperature on coal combustion characteristics, the change of char m/m_0 was analyzed, as shown in Figure 6. The char combustion process was enhanced with increase in oxygen temperature. When oxygen temperature was 300 K, most of the char could not finish combustion at the raceway outlet. More char reacted with oxygen with the increase in oxygen temperature. Furthermore, the char reaction rate significantly increased with the increase in oxygen temperature. This was mainly due to two reasons. On the one hand, the char combustion distance was extended. On the other hand, the coal particles got more heat with the increase in oxygen temperature. Moreover, the char combustion rate slowed at the end of the coal plume with the increase in oxygen temperature. This was mainly due to the lack of oxygen at the end of the raceway region.

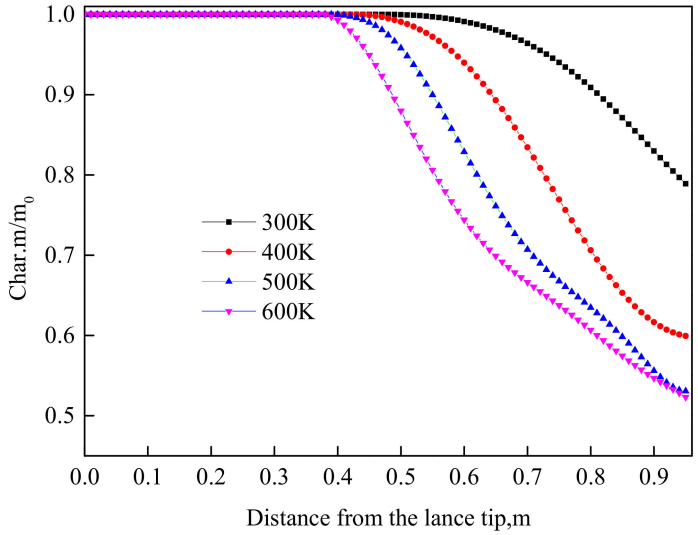

Figure 6. Effect of oxygen temperature on m/m_0 of char.

The oxygen distribution at different oxygen temperatures along Z = 0 plane was investigated, as shown in Figure 7. When the oxygen temperature was 300 K, a significant amount of oxygen was found at the raceway outlet. This further explains why most coal particles left the raceway region without full combustion. Less and less oxygen was found at the raceway outlet with the increase in oxygen temperature. When the oxygen temperature was 500 and 600 K, there was no oxygen at the raceway outlet. Oxygen therefore disappeared with the increase in oxygen temperature. This was closely related with char combustion. The coal combustion process was enhanced with the increase in oxygen temperature. Furthermore, the oxygen volume decreased with the increase in oxygen temperature. This further explains why the coal burnout increased slowly and the char combustion rate decreased at the end of the raceway region when the oxygen temperature was 500 and 600 K. When the oxygen temperature was 500 and 600 K, the oxygen concentration was the main factor affecting further coal combustion. The coal burnout would further increase by increasing oxygen concentration in the downstream of the coal plume. This is an important method for intensifying coal combustion in TGR-OBF.

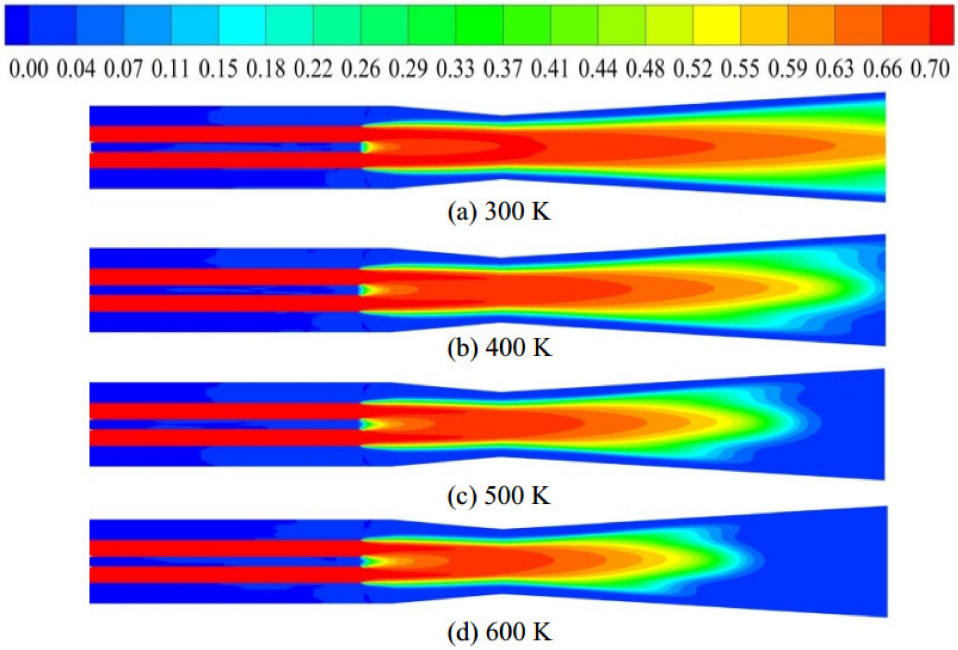

Figure 7. Effect of oxygen temperature on oxygen distributions along Z = 0 plane.

The gas temperature is closely related to reactions and reflects the relationship between reactions and heat transport. Therefore, the average gas temperature along the horizontal direction at different oxygen temperatures was investigated, as shown in Figure 8. In general, the average gas temperature in the first part of the raceway region increased with the increase in oxygen temperature. This was because the cold oxygen amount decreased as the oxygen temperature increased. The recycling gas and char combustion rate rapidly increased, and more heat was released. However, at the end of the raceway region, the average gas temperature at 400 K oxygen temperature was higher than that at other oxygen temperatures. Furthermore, the average gas temperature at 500 K oxygen temperature was higher than that at 300 and 600 K. The average gas temperature at 600 K oxygen temperature was higher than that at 300 K. The reasons for this can be explained as follows. As shown in Figures 4c and 6, the recycling gas and char combustion rate at 400 K oxygen temperature was higher than that of other temperatures at the end of the raceway. The means that more heat was released. Figure 7 shows the oxygen was completely consumed at the end of the raceway when the oxygen temperature was 500 and 600 K. This meant no more heat would be released. Furthermore, the endothermic reaction of char with CO_2 and H_2O would go on. Therefore, the gas temperature at 500 and 600 K oxygen temperature declined at the raceway outlet.

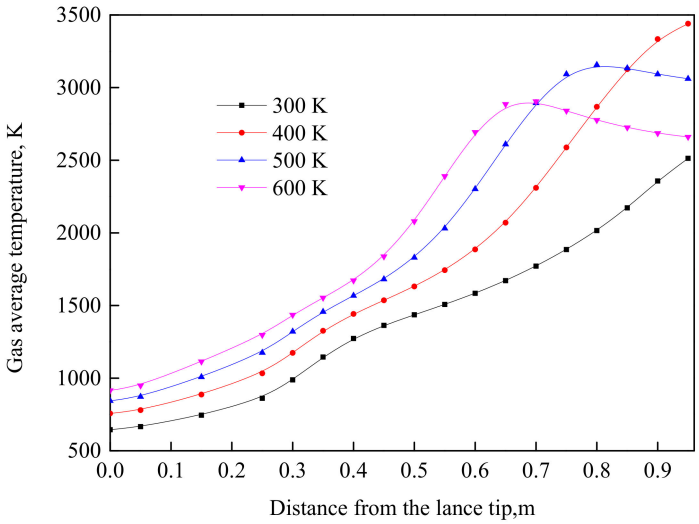

Figure 8. Effect of oxygen temperature on average gas temperature along the centerline.

4.3. Effect of Oxygen Temperature at the Same Mass Flow

To further understand the effect of oxygen stream, the effect of oxygen temperature at the same mass flow on coal combustion was investigated. Figure 9 shows the effect of oxygen temperature on the final coal burnout. In general, the coal burnout increased with the increase in oxygen temperature. However, the change was not very obvious. When the oxygen temperature increased to 400 K, the coal burnout increased to 26.99%, an increase of only 5.35%. When the oxygen temperature increased to 500 K, the coal burnout was 42.89%, an increase of 21.25% compared to that at 300 K. When the oxygen temperature was 600 K, the coal burnout was further increased. This was because more heat was brought in with the increase in oxygen temperature. Furthermore, the higher temperature promoted the combustion reaction of recycling gas, and more heat was released. However, the mass flow of cold oxygen remained the same, and the cooling effect of oxygen stream was still obvious.

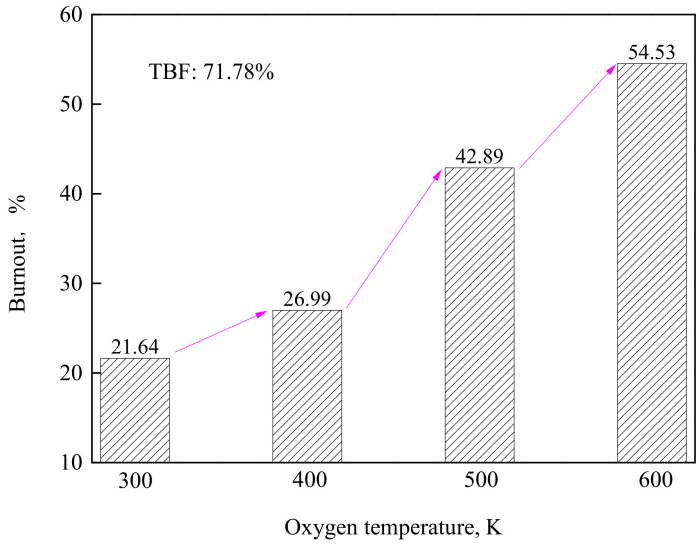

Figure 9. Effect of oxygen temperature on the final coal burnout.

Figure 10a shows the coal burnout at different distances from the lace tip under different oxygen temperatures. The coal particles released volatiles at almost the same distance from the lace tip under different oxygen temperatures. Furthermore, the coal burnout at different oxygen temperatures all maintained rapid growth, and the increasing rate became higher with the increase in oxygen temperature. The reasons causing this phenomenon can be explained as follows. The cooling effect

of the oxygen stream on devolatilization was still obvious. The recycling gas combustion reaction strengthened with the increase in oxygen temperature, and more heat was released. This made up for the hysteresis of the coal combustion process, but the effect was not very obvious. To further explore the reasons, the CO combustion rate along the centerline direction was investigated, as shown in Figure 10b. In the initial stage, the CO reaction rate increased significantly with the increase in oxygen temperature, and much heat was released. This was because the velocity of the oxygen stream increased significantly with the increase in oxygen temperature, and the mixing of oxygen and recycling gas increased. However, the coal particles got less heat. On the one hand, more cold oxygen shared more heat. On the other hand, the oxygen stream velocity increased with the increase in oxygen temperature. This was unfavorable for heat transfer to coal particles. In general, decreasing the cold oxygen amount in direct contact with coal particles and enhancing recycling gas combustion is the most effective method to increase coal burnout of TGR-OBF.

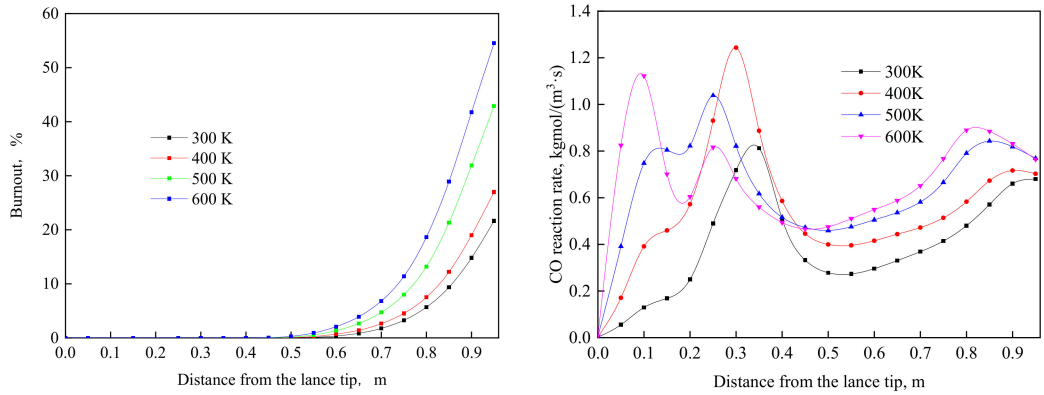

(a) (b)

Figure 10. Effect of oxygen temperature on (**a**) coal burnout at different positions; (**b**) CO combustion rate at different positions.

5. Conclusions

To further understand the effect of oxygen stream and intensify coal combustion in TGR-OBF, a three-dimensional model was developed to simulate the lance–blowpipe–tuyere–raceway of an TGR-OBF. The effect of oxygen temperature on coal combustion was investigated. The main conclusions are as follows.

(1) The cooling effect of room-temperature oxygen is the main reason causing a lower burnout in TGR-OBF. The coal burnout can be increased significantly by decreasing the cold oxygen volume in direct contact with coal particles. When the oxygen temperature increased from 300 to 500 K at the same velocity, the coal burnout was increased by 60.34%.

(2) The initial heat for coal combustion is from recycling gas combustion. The coal combustion process will be enhanced by improving recycling gas combustion. Increasing the mixing of recycling gas and oxygen will significantly promote the combustion reaction. This is an important method to increase coal burnout of TGR-OBF.

(3) When the oxygen temperature was 500 K at the same velocity, the coal combustion was weakened due to the lack of oxygen at the end of the raceway region. Increasing the oxygen content at the end of the raceway region is also an effective way to further increase coal burnout.

(4) Increasing oxygen temperature is very helpful for coal combustion. The preheating method of oxygen stream will be a very important research direction in future works. Furthermore, the way of injecting the oxygen stream also has a different effect on coal combustion. This is also the focus of future investigation.

Author Contributions: Investigation, Z.Z. and R.W.; data curation Q.Y.; writing—original draft preparation, Z.Z. and R.W.; writing—review and editing, G.W. and C.M. All authors have read and agreed to the published version of the manuscript.

Funding: This research was funded by the Natural Science Foundation of Shandong Province, grant number ZR2019BEE077.

Acknowledgments: The authors gratefully acknowledge the financial support provided by the Natural Science Foundation of Shandong Province (No. ZR2019BEE077).

Conflicts of Interest: The authors declare no conflict of interest. The funders had no role in the design of the study; in the collection, analyses, or interpretation of data; in the writing of the manuscript; or in the decision to publish the results.

References

1. Geerdes, M.; van Laar, R.; Vaynshteyn, R. Low-cost hot metal: The future of blast furnace ironmaking. *Iron Steel Technol.* **2011**, *8*, 51.
2. Chen, W.H.; Du, S.W.; Tsai, C.H.; Wang, Z.Y. Torrefied biomasses in a drop tube furnace to evaluate their utility in blast furnaces. *Bioresour. Technol.* **2012**, *111*, 433–438. [CrossRef]
3. Suopajarvi, H.; Pongracz, E.; Fabritius, T. Bioreducer use in Finnish blast furnace ironmaking–Analysis of CO_2 emission reduction potential and mitigation cost. *Appl. Energy* **2014**, *124*, 82–93. [CrossRef]
4. Ho, C.K.; Wu, S.M.; Zhu, H.P.; Yu, A.B.; Tsai, S.T. Experimental and numerical investigations of gouge formation related to blast furnace burden distribution. *Miner. Eng.* **2009**, *22*, 986–994. [CrossRef]
5. Arasto, A.; Tsupari, E.; Karki, J.; Lilja, J.; Sihvonen, M. Oxygen blast furnace with CO_2 capture and storage at an integrated steel mill—Part I: Technical concept analysis. *Int. J. Greenh. Gas Control* **2014**, *30*, 140–147. [CrossRef]
6. Sato, M.; Takahashi, K.; Nouchi, T.; Ariyama, T. Predictcion of Next-Generation Ironmaking Process Based on Oxygen Blast Furnace Suitable for CO_2 Mitigation and Energy Flexibility. *ISIJ Int.* **2015**, *55*, 2105–2114. [CrossRef]
7. Liu, L.; Jiang, Z.; Zhang, X.; Lu, Y.; He, J.; Wang, J.; Zhang, X. Effects of top gas recycling on in-furnace status, productivity, and energy consumption of oxygen blast furnace. *Energy* **2018**, *163*, 144–150. [CrossRef]
8. Zhang, W.; Zhang, J.; Xue, Z. Exergy analyses of the oxygen blast furnace with top gas recycling process. *Energy* **2017**, *121*, 135–146. [CrossRef]
9. Han, Y. *Fundamental Research on Ironmaking Process of Top Gas Recycling-Oxygen Blast Furnace*; University of Science and Technology Beijing: Beijing, China, 2012.
10. Dasireddy, V.D.; Stefancic, N.S.; Hus, M.; Likozar, B. Effect of alkaline earth metal oxide (MO) Cu/MO/Al_2O_3 catalysts on methanol synthesis activity and selectivity via CO_2 reduction. *Fuel* **2018**, *233*, 103–112. [CrossRef]
11. Marlin, D.S.; Sarron, E.; Sigurbjornsson, O. Process Advantages of Direct CO_2 to Methanol Synthesis. *Front. Chem.* **2018**, *6*, 446. [CrossRef]
12. Bobbink, F.D.; Menoud, F.; Dyson, P.J. Synthesis of Methanol and Diols from CO_2 via Cyclic Carbonates under Metal-Free, Ambient Pressure, and Solvent-Free Conditions. *ACS Sustain. Chem. Eng.* **2018**, *6*, 12119–12123. [CrossRef]
13. Zhou, Z.F.; Zhang, Y.Y.; Wang, G.; Wang, J.S.; Xue, Q.G. Investigation on Coal Combustion Behaviors in the Oxygen Blast Furnace. In *8th International Symposium on High-Temperature Metallurgical Processing*; Springer: San Diego, CA, USA, 2017; pp. 335–346.
14. Liu, Y.R.; Shen, Y.S. Computational Fluid Dynamics Study of Biomass Combustion in a Simulated Ironmaking Blast Furnace: Effect of the Particle Shape. *Energy Fuels* **2017**, *32*, 4372–4381. [CrossRef]
15. Shen, Y.S.; Yu, A.B. Modelling of injecting a ternary coal blend into a model ironmaking blast furnace. *Miner. Eng.* **2016**, *90*, 89–95. [CrossRef]
16. Shen, Y.S.; Yu, A.B.; Austin, P.R.; Zulli, P. CFD study of in-furnace phenomena of pulverised coal injection in blast furnace: Effects of operating conditions. *Powder Technol.* **2012**, *223*, 27–38. [CrossRef]
17. Du, S.W.; Yeh, C.P.; Chen, W.H.; Tsai, C.H.; Lucas, J.A. Burning characteristics of pulverized coal within blast furnace raceway at various injection operations and ways of oxygen enrichment. *Fuel* **2015**, *143*, 98–106. [CrossRef]
18. Du, S.W.; Chen, W.H.; Lucas, J. Performances of pulverized coal injection in blowpipe and tuyere at various operational conditions. *Energy Convers. Manag.* **2007**, *48*, 2069–2076. [CrossRef]

19. Yeh, C.P.; Du, S.W.; Tsai, C.H.; Yang, R.J. Numerical analysis of flow and combustion behavior in tuyere and raceway of blast furnace fueled with pulverized coal and recycled top gas. *Energy* **2012**, *42*, 233–240. [CrossRef]
20. Sahu, R.K.; Roy, S.K.; Sen, P.K. Applicability of top gas recycle blast furnace with downstream integration and sequestration in an integrated steel plant. *Steel Res. Int.* **2015**, *86*, 502–516. [CrossRef]
21. Helle, M.; Saxen, H. Operation Windows of the Oxygen Blast Furnace with Top Gas Recycling. *ISIJ Int.* **2015**, *55*, 2047–2055. [CrossRef]
22. Xuan, W.W.; Guan, Q.L.; Zhang, J.S. Kinetic model and CFD simulation for an entrained flow coal hydrogasifier and influence of structural parameters. *Int. J. Hydrogen Energy* **2016**, *41*, 20023–20035. [CrossRef]
23. Llbas, M.; Karyeyen, S. A numerical study on combustion behaviours of hydrogen-enriched low calorific value coal gases. *Int. J. Hydrogen Energy* **2015**, *40*, 15218–15226.
24. Zhou, Z.F.; Xue, Q.G.; Li, C.L.; Wang, G.; She, X.F.; Wang, J.S. Coal flow and combustion characteristics under oxygen enrichment way of oxygen-coal double lance. *Appl. Therm. Eng.* **2017**, *123*, 1096–1105. [CrossRef]
25. Zhou, Z.F.; Huo, H.L.; Wang, G.; Xue, Q.G.; She, X.F.; Wang, J.S. Effect of Oxygen-Coal Lance Configurations on Coal Combustion Behavior. *Steel Res. Int.* **2017**, *88*, 1600197. [CrossRef]
26. Zhou, Z.F.; Liu, Y.L.; Wang, G.; She, X.F.; Xue, Q.G.; Wang, J.S. Effect of Local Oxygen-enrichment Ways of Oxygen-coal Double Lance on Coal Combustion. *ISIJ Int.* **2017**, *57*, 279–285. [CrossRef]
27. Shen, Y.S.; Maldonado, D.; Guo, B.Y.; Yu, A.B.; Austin, P.; Zulli, P. Computational fluid dynamics study of pulverized coal combustion in blast furnace raceway. *Ind. Eng. Chem. Res.* **2009**, *48*, 10314–10323. [CrossRef]
28. Wijayanta, A.T.; Alam, M.S.; Nakaso, K.; Fukai, J.; Kunitomo, K.; Shimizu, M. Combustibility of biochar injected into the raceway of a blast furnace. *Fuel Process. Technol.* **2014**, *117*, 53–59. [CrossRef]
29. Ou, Z.S.; Jin, H.; Ren, Z.H.; Zhu, S.X.; Song, M.M.; Guo, L.J. Mathematical model for coal conversion in supercritical water: Reacting multiphase flow with conjugate heat transfer. *Int. J. Hydrogen Energy* **2018**, *44*, 15746–15757. [CrossRef]
30. Jin, H.H.; Xu, B.N.; Li, H.Q.; Ku, X.K.; Fan, J.R. Numerical investigation of coal gasification in supercritical water with the ReaxFF molecular dynamics method. *Int. J. Hydrogen Energy* **2018**, *43*, 20513–20524. [CrossRef]
31. Shen, Y.S.; Yu, A.B. Characterization of Coal Burnout in the Raceway of an Ironmaking Blast Furnace. *Steel Res. Int.* **2015**, *86*, 604–611. [CrossRef]
32. Wang, J.; Lou, H.H.; Yang, F.; Cheng, F. Numerical simulation of a decoupling and Re-burning combinative Low-NOx coal grate boiler. *J. Clean. Prod.* **2018**, *188*, 977–988. [CrossRef]
33. Baum, M.M.; Street, P.J. Predicting the combustion behaviour of coal particles. *Combust. Sci. Technol.* **1971**, *3*, 231–243. [CrossRef]